

Phytotoxic Effects of Mercuric Chloride on Growth, Chlorophyll Content, and Survival of *Paspalum scrobiculatum*

Aishwarya Senthil Kumar¹, Vijayalakshmi Srinivasan^{1*}

¹MCTM Chidambaram Chettyar International School, 179, Luz Church Road, Mylapore, Chennai – 600 004, Tamil Nadu, India.

*Corresponding Author

Dr Vijayalakshmi Srinivasan

Faculty, Department of Biology, MCTM Chidambaram Chettyar International School, 179, Luz Church Road, Mylapore, Chennai – 600 004, Tamil Nadu, India.

ABSTRACT

Mercury is among the most toxic heavy metals, exerting severe effects on plant growth and physiology. Understanding how plants respond to mercury stress is crucial for assessing ecological risk and developing remediation strategies. This study aimed to evaluate the impact of varying HgCl₂ concentrations on root and shoot length, chlorophyll content, and biomass of *Paspalum scrobiculatum*. Seedlings were exposed to 0.01, 0.02, 0.05, 0.07, and 0.10 ppm HgCl₂ concentrations for 14 days under controlled conditions. Root and shoot length were measured using a digital scale, chlorophyll content was quantified spectrophotometrically, and biomass parameters were recorded. HgCl₂ exposure caused a concentration-dependent decline in growth, chlorophyll content, biomass, and survival of *Paspalum scrobiculatum*. Shoot length decreased from 13.6 ± 0.3 cm in controls to 1.5 ± 0.2 cm at 0.10 ppm, while root length declined from 1.97 ± 0.20 cm to 0.50 ± 0.10 cm. Total chlorophyll content dropped sharply from 1.67 ± 0.04 to 0.36 ± 0.05 mg/g FW. Strong negative correlations ($r = -0.9$ to -1.0) were observed between HgCl₂ concentration and all growth and chlorophyll parameters. Fresh and dry biomass decreased by 59 % and 67 %, respectively, with a concomitant rise in tissue water content. Survival declined to 50 % at 0.10 ppm. Regression modeling estimated EC₅₀ values of 0.030–0.069 ppm across endpoints. Mercury stress in *P. scrobiculatum* impairs growth, pigment retention, and biomass allocation by disrupting cellular metabolism and promoting oxidative damage.

Keywords: Mercury toxicity, *Paspalum scrobiculatum*, Chlorophyll degradation, Biomass reduction, Heavy metal stress

1. INTRODUCTION

Environmental pollution has become one of the most pressing challenges of the 21st century, with anthropogenic activities contributing substantially to the degradation of ecosystems. Rapid industrialization, urbanization, intensive agriculture, and unregulated waste disposal have introduced a wide spectrum of chemical pollutants into air, water, and soil systems [1-3]. Among these, heavy metals and metalloids are of particular concern due to their persistence, non-biodegradability, and ability to bioaccumulate in living organisms [4]. Unlike many organic pollutants, heavy metals cannot be degraded and therefore remain in the environment for extended periods, cycling between soil, water, and biota, ultimately entering the human food chain [5]. Agricultural soils, in particular, are highly vulnerable to contamination because they act as sinks for pollutants originating from industrial effluents, mining activities, sewage sludge application, agrochemicals, and atmospheric deposition [6]. Elevated levels of toxic metals such as cadmium (Cd), lead (Pb), mercury (Hg), arsenic (As), and chromium (Cr) have been reported to impair soil fertility, alter microbial activity, and significantly reduce crop productivity [7]. The adverse impacts on plants include inhibition of seed germination, stunted growth, chlorosis, reduced photosynthetic efficiency, and in severe cases, plant death [8]. The consumption of contaminated plant products further poses serious health risks to humans, including neurotoxicity, carcinogenicity, and disruption of endocrine and immune functions [9].

Mercury is among the most hazardous heavy metals, classified as a global priority pollutant due to its extreme toxicity and mobility in the environment [10,11]. It exists in multiple forms—elemental (Hg^0), inorganic (Hg^{2+}), and organic (methylmercury)—each with distinct toxicological properties [12]. Inorganic mercuric chloride (HgCl_2), commonly used in

industrial applications such as leather processing, wood preservation, and disinfectants, is highly soluble in water, enabling its rapid entry into soil and aquatic systems [13]. Once in the soil, mercury is readily absorbed by plant roots, translocated to shoots, and accumulated in edible parts. Its phytotoxic effects are multifaceted, including disruption of chlorophyll synthesis, inhibition of photosystem function, interference with nutrient uptake, and induction of oxidative stress through the generation of reactive oxygen species (ROS) [14,15]. One of the key mechanisms of mercury-induced photosynthetic inhibition is the displacement of magnesium in the chlorophyll porphyrin ring, leading to altered pigment structure and reduced light-harvesting capacity [16]. Additionally, mercury binds strongly to sulfhydryl groups in enzymes and membrane proteins, impairing metabolic pathways and damaging chloroplast ultrastructure [17]. Even at low concentrations, mercury can cause substantial physiological damage, while higher levels may result in complete growth suppression or mortality in sensitive plant species.

Kodo millet (*Paspalum scrobiculatum* L.) is an underutilized cereal crop widely cultivated in semi-arid and marginal regions of South Asia, particularly in southern India [18]. It is valued for its nutritional profile, being rich in fiber, essential amino acids, and minerals, and its resilience to drought and poor soils [19]. Millets are increasingly promoted as climate-smart crops, offering a sustainable alternative to water- and nutrient-intensive cereals like rice and wheat. However, their cultivation in contaminated soils raises significant food safety concerns, as the accumulation of heavy metals in edible grains can compromise both human health and marketability.

Despite the global attention on heavy metal toxicity in staple crops, there is limited research on the effects of mercury on millets, particularly kodo millet. Given the rising levels of environmental contamination in agricultural regions and the absence of comprehensive phytotoxicity data for this crop, it is essential to investigate how varying concentrations of

mercury affect its growth and physiological performance. Such studies not only provide insights into plant tolerance and sensitivity mechanisms but also inform strategies for mitigating contamination risks in food systems. The current study intends to evaluate the concentration-dependent effects of HgCl_2 on growth, chlorophyll pigment content, and biomass production of *P. scrobiculatum*.

2. METHODOLOGY

2.1 Plant Material and Growth Conditions

Seeds of *P. scrobiculatum* were sourced locally. Seeds were surface sterilized by soaking in distilled water for 24 h, drained, and incubated in a closed container with perforations until 5 days or till germination was observed. Uniformly sprouted seedlings were selected for experiments. Plants were grown in 500 mL plastic containers filled with 80 g of moistened cocopeat (Fig. 1). Growth conditions were maintained at 25 ± 2 °C, relative humidity 60–70%, and photoperiod of 12 h light / 12 h dark under a light intensity of 180 ± 10 $\mu\text{mol photons m}^{-2} \text{s}^{-1}$. Containers were positioned randomly within the growth area and rotated daily to minimize positional bias. Aeration was maintained by drilling six holes at the base of each container, and all plants received equal watering to maintain consistent moisture.



Fig. 1. Experimental setup showing *Paspalum scrobiculatum* seedlings grown under varying concentrations of HgCl_2 treatments in controlled pot culture conditions.

2.2 Mercuric Chloride Treatments

Analytical-grade HgCl₂ powder was used to prepare treatment solutions. Six concentrations were tested: 0 (control), 0.01, 0.025, 0.05, 0.075, and 0.1 ppm. Concentrations were chosen to represent sub-permissible to supra-permissible levels relative to the FAO-reported safe limit of 0.02 ppm for agricultural soils. All measuring devices were calibrated before solution preparation. Each treatment was applied daily by pouring 25 mL of the respective solution evenly along the sides of the container. Control plants received distilled water. The experiment followed a completely randomized design with five biological replicates per treatment. Each replicate consisted of 10 seedlings grown in a separate container. The exposure period was 14 days. All measurements were conducted at harvest.

2.3 Growth and Biomass Measurements

At harvest, plants were carefully removed from cocopeat, washed under tap water, and blot-dried. Root length was measured from the stem base to the root tip. Shoot length was measured from the stem base to the shoot tip. Measurements were taken using a stainless-steel ruler (± 0.1 cm), calibrated before use. In addition to length measurements, Fresh biomass (FB) of each replicate was recorded immediately using a precision balance (± 0.001 g). Dry biomass (DB) was obtained by oven-drying the same samples at 65 °C for 72 h, or until constant mass was achieved (two consecutive weighings differing by < 1 mg after an additional 3 h of drying). All biomass measurements were carried out in grams (g). Derived water status indices including dry matter content (DMC, %) and water content (WC, % of fresh) were calculated by.

$$\text{Dry matter content (DMC)} = 100 \times \frac{\text{Dry biomass}}{\text{Fresh biomass}}$$

$$\text{Water content (WC)} = 100 \times \frac{\text{Fresh biomass} - \text{Dry biomass}}{\text{Fresh biomass}}$$

2.4 Chlorophyll and Survival Rate Estimation

Chlorophyll was extracted by using the method of Lee et al., (2021) [20]. Briefly, fresh 0.2 g shoot tissue was homogenized in 90 % acetone using a mortar and pestle, and the extract was centrifuged at 3000 rpm for 5 min. The supernatant was collected, and absorbance was measured at 645 nm and 663 nm using a UV-Vis spectrophotometer (± 0.001 A), calibrated against a 90 % acetone blank before each reading. The total chlorophyll (mg/g fresh weight) was calculated as:

$$\text{Total chlorophyll} = \frac{[20.2 \times A_{645} + 8.02 \times A_{663}] \times V}{100 \times W}$$

Where: V = extract volume, W = fresh tissue weight

Survival rate was estimated as:

$$\text{Survival rate (\%)} = \frac{\text{Number of live plants}}{\text{total plants}} \times 100$$

A plant was considered alive if its shoot was green and upright at the end of the 14-day exposure.

2.5 Statistical Analysis

Data were expressed as mean \pm standard deviation (SD) of biological replicates. Pearson's correlation coefficients (r) were calculated between HgCl_2 concentration and measured parameters (root length, shoot length, biomass, chlorophyll content, survival rate). Relationships were further evaluated via regression analysis (best-fit models reported with R^2 values). Treatment effects on root length, shoot length, biomass, and chlorophyll parameters were evaluated using one-way multivariate analysis of variance (MANOVA). Statistical significance was set at $p < 0.05$. All analyses were performed using Microsoft Excel 365 and R v4.5.1. EC_{50} values were estimated with a four-parameter log-logistic model (LL.4) on responses normalized to % control; 0-dose points were excluded from fitting (log-scale). We report delta-method 95% CIs.

3. RESULTS

Exposure of *P. scrobiculatum* seedlings to increasing concentrations of HgCl₂ for 14 days resulted in a concentration-dependent reduction in both root and shoot length (Table 1) (Fig. 2). Mean final shoot length in the control group was 13.6 ± 0.3 cm, which decreased significantly ($p < 0.05$) to 1.5 ± 0.2 cm at 0.1 ppm HgCl₂ (Fig. 3). Similarly, mean final root length decreased from 1.97 ± 0.20 cm in control plants to 0.50 ± 0.10 cm at 0.1 ppm HgCl₂. The most pronounced reductions were observed at concentrations ≥ 0.05 ppm (Fig. 4).



Fig. 2. Representative seedlings of *P. scrobiculatum* after 14 days of exposure to different HgCl₂ concentrations. The diagram illustrates the progressive reduction in shoot and root length at higher HgCl₂ concentrations.

Table 1: Mean final root length, shoot length, and percentage change relative to control in *P. scrobiculatum* after 14 days of HgCl₂ exposure.

HgCl ₂ (ppm)	Final RL (cm)	%Δ RL	Final SL (cm)	%Δ SL
Control	1.97 ± 0.20	240.04	13.6 ± 0.3	273.13
0.010	1.70 ± 0.20	137.15	9.9 ± 0.3	175.96
0.025	1.64 ± 0.20	163.29	6.9 ± 0.3	118.56
0.050	1.31 ± 0.20	54.32	3.2 ± 0.3	54.73
0.075	0.82 ± 0.20	22.86	2.5 ± 0.3	39.26
0.100	0.50 ± 0.10	16.60	1.5 ± 0.2	23.00

Values are **mean** \pm **SD** (n = 5 trials per treatment). RL = root length; SL = shoot length.

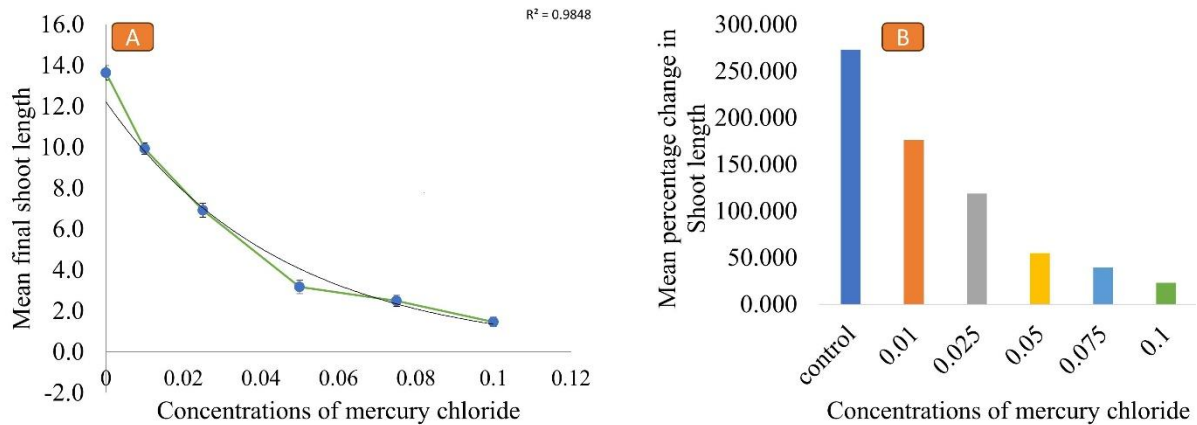


Fig. 3. A) Mean final shoot length at varying concentrations of HgCl₂ and B) Mean percentage change of shoot length at varying concentrations of HgCl₂.

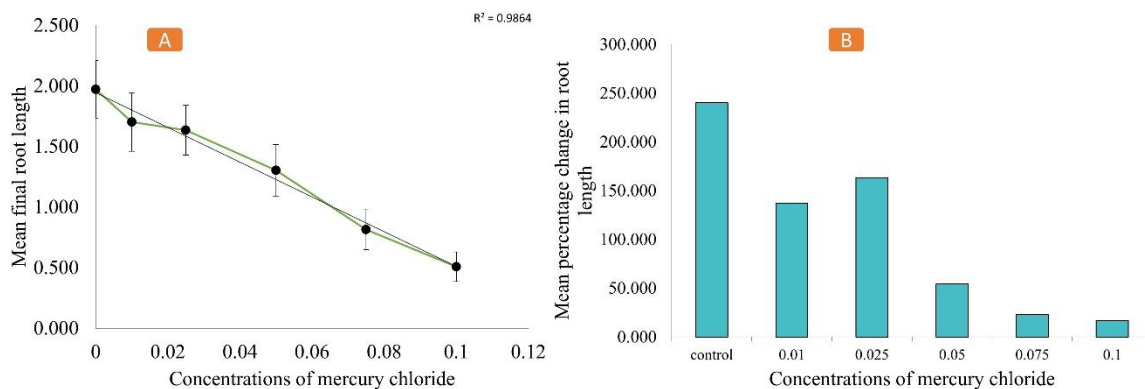


Fig. 4. A) Mean final root length at varying concentrations of HgCl₂ and B) Mean percentage change of root length at varying concentrations of HgCl₂.

Total chlorophyll content exhibited a strong negative correlation ($r = -1.00$) with HgCl₂ concentration. Control plants had 1.67 ± 0.04 mg/g FW total chlorophyll, while plants at 0.1 ppm contained only 0.36 ± 0.05 mg/g FW (Table 2). A slight increase was observed at 0.025 ppm compared to 0.01 ppm, suggesting a possible hormetic response at low exposure levels (Table 2). Survival rate also declined with increasing HgCl₂ concentration (Table 2). Control plants showed 88 ± 8.37 % survival, whereas only 50 ± 10.0 % survived at 0.1 ppm. The mean

total chlorophyll content and survival rate for varying concentrations of HgCl₂ is presented in Figure 5.

Table 2: Effect of HgCl₂ on total chlorophyll content and survival rate of *P. scrobiculatum* (14-day exposure).

HgCl ₂ (ppm)	Total chlorophyll (mg·g ⁻¹ FW)	Survival rate (%)
Control	1.67 ± 0.039	88.0 ± 8.37
0.010	1.58 ± 0.014	82.0 ± 4.47
0.025	1.56 ± 0.021	72.0 ± 8.37
0.050	0.90 ± 0.012	66.0 ± 5.48
0.075	0.49 ± 0.015	56.0 ± 8.94
0.100	0.36 ± 0.052	50.0 ± 10.0

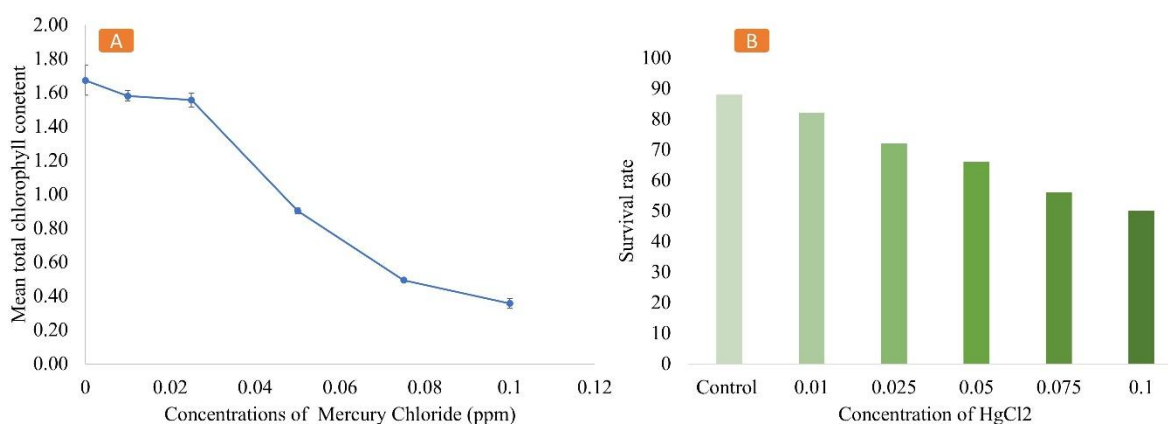


Fig. 5. A) Mean Total chlorophyll content B) survival rate for varying concentrations of HgCl₂.

FB declined progressively with increasing HgCl₂ concentration (Table 3). Control plants exhibited a mean FB of 1.82 ± 0.06 g, whereas seedlings exposed to 0.10 ppm averaged only 0.74 ± 0.05 g (a 59.3 % reduction; $p < 0.001$). The decline was detectable from 0.025 ppm (15.9 % lower than control, $p = 0.021$) and became pronounced at ≥ 0.050 ppm ($p < 0.001$). The DB showed a similar but steeper concentration–response trend, falling from 0.49 ± 0.02 g in the control to 0.16 ± 0.01 g at 0.10 ppm (a 67.3 % reduction; $p < 0.001$). Correspondingly, DMC decreased from 26.9 ± 0.6 % (control) to 21.3 ± 0.7 % at the highest concentration ($p < 0.01$), suggesting impaired carbon assimilation and allocation under mercury stress. WC

increased slightly but significantly with HgCl₂ concentration ($r = +0.88$, $p = 0.021$), rising from 73.1 ± 0.6 % in controls to 78.7 ± 0.7 % at 0.10 ppm, indicative of reduced structural biomass relative to water mass.

Table 3: Effect of HgCl₂ on biomass and derived indices in *P. scrobiculatum* seedlings (mean \pm SD, n = 5).

HgCl ₂ (ppm)	Fresh biomass (g)	Dry biomass (g)	DMC (%)	WC (%)
0.000	1.82 \pm 0.06	0.49 \pm 0.02	26.9 \pm 0.6	73.1 \pm 0.6
0.010	1.74 \pm 0.07	0.47 \pm 0.03	26.8 \pm 0.8	73.2 \pm 0.8
0.025	1.53 \pm 0.08	0.41 \pm 0.02	26.7 \pm 0.7	73.3 \pm 0.7
0.050	1.15 \pm 0.05	0.29 \pm 0.01	25.2 \pm 0.5	74.8 \pm 0.5
0.075	0.92 \pm 0.06	0.22 \pm 0.01	23.9 \pm 0.6	76.1 \pm 0.6
0.100	0.74 \pm 0.05	0.16 \pm 0.01	21.3 \pm 0.7	78.7 \pm 0.7

Pearson's correlation analysis demonstrated strong and statistically significant negative associations between HgCl₂ concentration and all measured physiological parameters. Specifically, root length exhibited a correlation coefficient of $r = -0.90$ ($p < 0.01$), indicating that as HgCl₂ concentration increased, root elongation decreased markedly. A similar trend was observed for shoot length ($r = -0.90$, $p < 0.01$), reflecting substantial growth inhibition in the aerial parts of the plants. Total chlorophyll content showed the strongest relationship, with a perfect negative correlation of $r = -1.00$ ($p < 0.01$), suggesting that chlorophyll degradation was almost entirely concentration-dependent. With respect to biomass a strong negative relationship between HgCl₂ concentration and FB ($r = -0.94$, $p < 0.01$) and DB ($r = -0.96$, $p < 0.01$), and a weaker but significant negative correlation with DMC ($r = -0.82$, $p = 0.046$) was observed. WC was positively correlated with concentration ($r = +0.88$, $p = 0.021$). These relationships are visualized in Figure 6 as a correlation heatmap, which highlights the uniform and strong inverse trends across all parameters

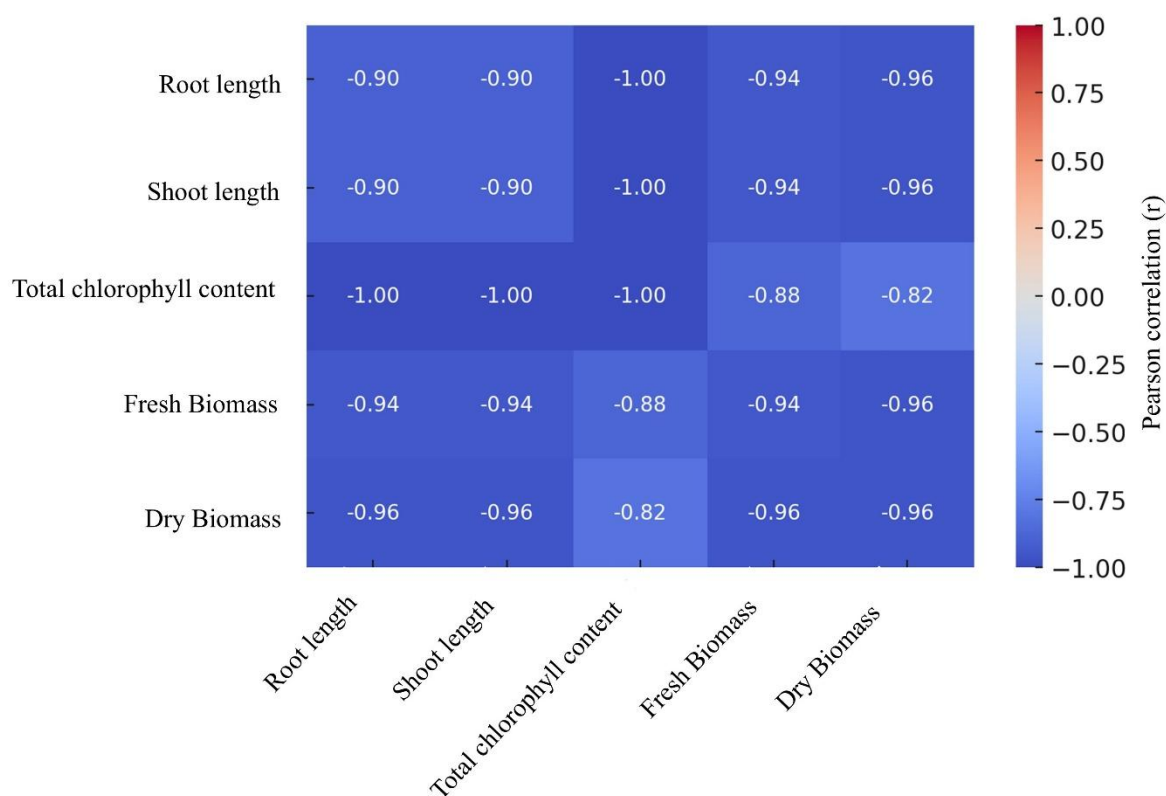


Fig. 6. Correlation heatmap depicting HgCl_2 concentration vs plant parameters.

Regression modelling revealed that the observed reductions followed exponential decay patterns for all three parameters. For shoot length, the model explained 98.48 % of the variance ($R^2 = 0.9848$), while root length exhibited an equally strong model fit with $R^2 = 0.9864$. The regression for total chlorophyll content accounted for 95.56 % of the variance ($R^2 = 0.9556$), further supporting the high predictability of parameter decline with increasing HgCl_2 concentration. These results collectively indicate that HgCl_2 exerts a pronounced, quantifiable, and concentration-dependent inhibitory effect on plant growth and pigment retention.

The MANOVA analysis yielded a statistically significant overall effect of HgCl_2 treatment on the dependent variables (Pillai's trace = 1.613, $F(15, 72) = 5.58$, $p = 2.394 \times 10^{-7}$, partial $\eta^2 = 0.54$). This result indicates that 54 % of the total variance in the combined outcome measures could be attributed to differences in HgCl_2 concentration. The significant MANOVA outcome corroborates the univariate findings, confirming that mercury exposure simultaneously and adversely influences multiple aspects of plant physiological performance.

The dose–response modelling using a four-parameter logistic regression revealed clear differences in the sensitivity of measured parameters to HgCl_2 exposure. For root length, the estimated EC_{50} value was 0.069 ppm (95 % CI: 0.044–0.095) with a Hill slope of -2.44 , indicating a marked decline in growth at relatively low concentrations. Shoot length showed an EC_{50} of 0.030 ppm (95 % CI: -0.017 – 0.077) with a Hill slope of -5.62 ; however, this estimate was unstable and associated with a wide confidence interval, likely due to the steep decline and limited number of intermediate concentration points. Total chlorophyll content exhibited the highest sensitivity to HgCl_2 , with an EC_{50} of 0.048 ppm (95 % CI: 0.030–0.066) and a Hill slope of -4.26 , reflecting a strong inhibitory effect even at sub-lethal concentrations. Among the measured endpoints, chlorophyll content provided the most robust EC_{50} estimate, whereas shoot length required further data refinement or model simplification for improved precision. Figure 7 presents the fitted dose–response curves with 95% confidence intervals and EC_{50} thresholds for each parameter.

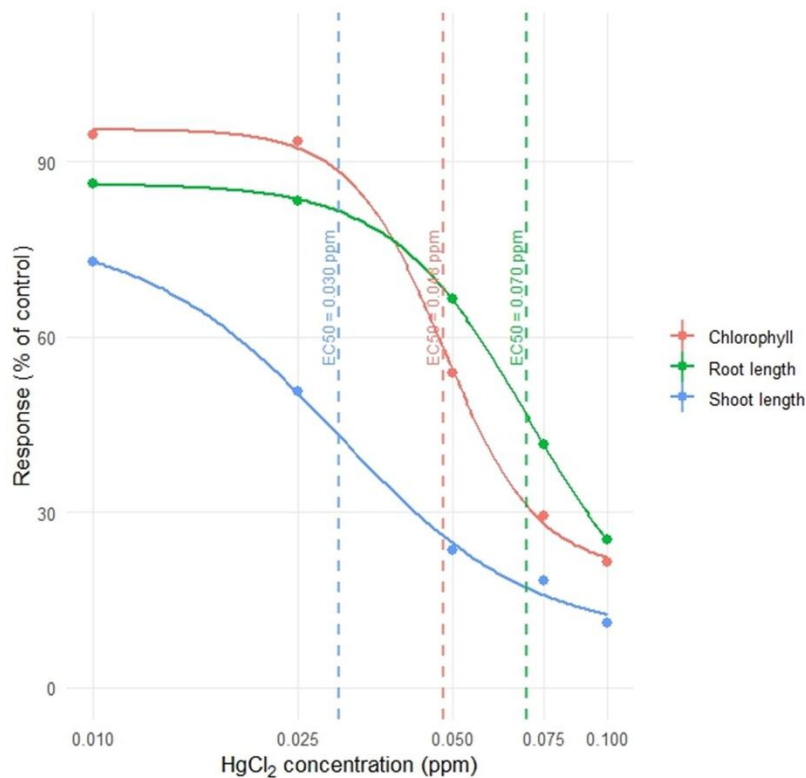


Fig. 7. Dose response curves for root length, shoot length, and total chlorophyll content in *P. scrobiculatum* seedlings exposed to increasing concentrations of HgCl₂. Data points represent the mean \pm SD as percentage of control.

4. DISCUSSION

The present study clearly demonstrates that exposure of *P. scrobiculatum* seedlings to increasing concentrations of HgCl₂ induces pronounced and progressive growth inhibition, chlorophyll degradation, and biomass loss. The observed reduction in both root and shoot length across treatments aligns with the well-documented phytotoxic effects of mercury on higher plants. Mercury is a highly reactive heavy metal that readily binds to sulfhydryl (-SH) groups in proteins, altering their structure and inactivating critical enzymes involved in cellular metabolism [21]. This interference extends to enzymes involved in cell wall loosening and expansion, thereby directly constraining cell elongation and differentiation in the growing zones of both roots and shoots [22]. The more marked inhibition observed at concentrations ≥ 0.05 ppm suggests that beyond a certain threshold, the detoxification and repair mechanisms of the plant become overwhelmed, leading to rapid growth arrest.

Roots, as the primary site of contact with mercury in the growth medium, are more directly exposed to toxic ionic species. The reduction in root length in our study may be attributed to direct injury to the root apical meristem and disruption of auxin gradients essential for elongation [23]. Mercury has been shown to impair auxin transport by binding to thiol groups in transport proteins and by generating ROS that degrade hormone molecules [24]. Furthermore, mercury-induced ROS accumulation can damage membrane lipids, proteins, and nucleic acids in meristematic cells, reducing their viability and capacity to divide [25]. Once root uptake is compromised, translocation of water and nutrients to the shoot is hindered, amplifying the inhibitory effects on shoot elongation [26]. This explains the parallel decline in aerial growth observed in the seedlings, as reduced nutrient and water availability, combined

with direct mercury toxicity to shoot tissues, limits expansion of leaf blades and internodes [14].

The strong decline in total chlorophyll content across treatments indicates that mercury toxicity extends beyond structural growth inhibition to directly impair photosynthetic capacity. Chlorophyll degradation under heavy metal stress is a well-documented phenomenon, with several converging mechanisms. Mercury can directly inhibit the activity of δ -aminolevulinic acid dehydratase and protochlorophyllide reductase, key enzymes in the chlorophyll biosynthetic pathway [27,28]. Additionally, mercury disrupts the thylakoid membrane structure by displacing essential cations such as Mg^{2+} , which is centrally coordinated in the chlorophyll molecule, and by enhancing lipid peroxidation through ROS production [14,15,29]. The high correlation between $HgCl_2$ concentration and chlorophyll loss in our study suggests that pigment breakdown is not only a consequence of oxidative damage but also of direct metabolic inhibition. The slight increase in chlorophyll content at 0.025 ppm compared with 0.01 ppm reflects a low-dose hormetic response, wherein mild stress triggers upregulation of antioxidant enzymes and pigment synthesis pathways as an adaptive mechanism [30]. However, such stimulation is transient and reverses as stress intensity rises, as seen at higher mercury concentrations in our results.

Biomass measurements provide further understanding into the physiological toll exerted by mercury exposure. The observed reductions in FB and DB suggest that $HgCl_2$ interferes with both carbon assimilation and the allocation of assimilates to structural components [31]. Reduced photosynthetic pigment content naturally leads to lower photosynthetic rates, which in turn limit the supply of carbohydrates necessary for growth and biomass accumulation. Mercury's interference with photosystem II electron transport and Calvin cycle enzymes, as demonstrated in other grass species [32], likely further constrains carbon fixation. The more pronounced decline in DB relative to FB in our study, alongside with the increase WC, indicates

a shift towards tissues with higher water proportion and reduced structural density. This pattern may result from weakened cell walls due to inhibition of cellulose and lignin biosynthesis under mercury stress [33]. Inhibition of phenylalanine ammonia-lyase, a key enzyme in the phenylpropanoid pathway, by heavy metals has been reported to reduce lignin deposition, leading to softer, more water-rich tissues [34]. The increase in WC observed with rising HgCl₂ concentration may also represent a stress adaptation strategy. Higher cellular water content can help maintain turgor pressure despite impaired cell wall rigidity, potentially delaying wilting under stress [35]. However, this comes at the cost of reduced mechanical strength and lower dry matter content, which could compromise plant survival in natural environments and reduce the quality of harvested biomass in agricultural settings. A reduction in DMC from 26.9 % to 21.3 % as observed here reflects not only lower carbon deposition but also changes in osmotic balance, with mercury-induced accumulation of compatible solutes such as proline and soluble sugars contributing to osmotic adjustment [29,36]. The simultaneous impairment of root elongation, shoot elongation, chlorophyll retention, and biomass accumulation suggests that mercury toxicity acts through multiple, interconnected physiological pathways rather than a single target. ROS overproduction appears to be a central mechanism, as mercury exposure is known to inhibit antioxidant enzymes such as superoxide dismutase, catalase, and ascorbate peroxidase, leading to oxidative stress [37,38].

Published literature supports the view that chlorophyll degradation often precedes visible symptoms of growth inhibition, making it a sensitive early indicator of heavy metal toxicity. In rice (*Oryza sativa*), for example, Hg exposure has been shown to cause significant chlorophyll loss within days, even before marked reductions in leaf area or biomass are observed [39]. The sensitivity of chlorophyll content in our study, where it declined sharply even at sub-lethal concentrations, mirrors these findings and underscores its potential as a biomarker for early detection of mercury stress in grasses.

Our results also contribute to understanding species-specific responses to mercury. While *P. scrobiculatum* shows clear sensitivity at concentrations as low as 0.025 ppm for some parameters, other grass species such as *Lolium perenne* have been reported to tolerate higher mercury levels before exhibiting similar declines [40]. This variability may be attributed to differences in root exudate composition, cell wall binding capacity for heavy metals, and efficiency of phytochelatin synthesis [41]. Phytochelatins are small, cysteine-rich peptides that chelate heavy metals and sequester them into vacuoles, thereby reducing their cytoplasmic toxicity. However, excessive mercury may saturate this system, leading to free ionic mercury accumulation and consequent damage. The steep declines we observed at higher concentrations suggest that *P. scrobiculatum*'s detoxification capacity is limited, making it more vulnerable to mercury than some other grasses.

5. CONCLUSION

The present study demonstrates that HgCl₂ exerts a strong, concentration-dependent inhibitory effect on the growth and physiology of *P. scrobiculatum*. Reductions in shoot and root elongation, chlorophyll content, and biomass, coupled with increased tissue water content, highlight the disruption of photosynthetic efficiency and carbon allocation under mercury stress. The low EC₅₀ thresholds indicate high sensitivity of this species even at sub-lethal concentrations, underscoring its vulnerability to mercury contamination. Collectively, these findings not only provide mechanistic insights into mercury-induced phytotoxicity but also support the potential use of *P. scrobiculatum* as a sensitive bioindicator for monitoring mercury pollution in agricultural and natural ecosystems.

While the present findings clearly establish the concentration-dependent toxicity of HgCl₂ in *P. scrobiculatum*, they are limited by the controlled laboratory setting and short exposure duration. Future studies incorporating long-term trials, multiple species, and molecular

analyses will be essential to validate these patterns and guide phytoremediation and crop resilience strategies in mercury-contaminated ecosystems.

Conflict of Interests

On behalf of all authors, the corresponding author states that there is no conflict of interest.

Availability of data and materials

Available on request.

REFERENCES

1. Akhtar, N., Syakir Ishak, M.I., Bhawani, S.A., Umar, K., 2021. Various natural and anthropogenic factors responsible for water quality degradation: a review. *Water*, 13(19), 2660.
2. Khanam, Z., Sultana, F.M., Mushtaq, F., 2023. Environmental pollution control measures and strategies: an overview of recent developments. In: *Geospatial Analytics for Environmental Pollution Modeling: Analysis, Control and Management*, pp. 385–414.
3. Durdu, B., Gurbuz, F., Koçyiğit, H., Gurbuz, M., 2023. Urbanization-driven soil degradation; ecological risks and human health implications. *Environmental Monitoring and Assessment*, 195(8), 1002.
4. Edo, G.I., Samuel, P.O., Oloni, G.O., Ezekiel, G.O., Ikpekoru, V.O., Obasohan, P., Ongulu, J., Otunuya, C.F., Opiti, A.R., Ajakaye, R.S., Essaghah, A.E., 2024. Environmental persistence, bioaccumulation, and ecotoxicology of heavy metals. *Chemical Ecology*, 40(3), 322–349.
5. Emenike, E.C., Iwuozor, K.O., Anidiobi, S.U., 2022. Heavy metal pollution in aquaculture: sources, impacts and mitigation techniques. *Biological Trace Element Research*, 200(10), 4476–4492.
6. Shakti, P., Pandey, A.K., 2024. Agricultural soil contamination due to industrial discharges: challenges for public health protection and food security. In: *Bioremediation of Emerging Contaminants from Soils*. Elsevier, pp. 21–42.
7. Rashid, A., Schutte, B.J., Ulery, A., Deyholos, M.K., Sanogo, S., Lehnhoff, E.A., Beck, L., 2023. Heavy metal contamination in agricultural soil: environmental pollutants affecting crop health. *Agronomy*, 13(6), 1521.
8. Seneviratne, M., Rajakaruna, N., Rizwan, M., Madawala, H.M., Ok, Y.S., Vithanage, M., 2019. Heavy metal-induced oxidative stress on seed germination and seedling development: a critical review. *Environmental Geochemistry and Health*, 41(4), 1813–1831.
9. Munir, N., Jahangeer, M., Bouyahya, A., El Omari, N., Ghchime, R., Balahbib, A., Aboulaghras, S., Mahmood, Z., Akram, M., Ali Shah, S.M., Mikolaychik, I.N., 2021. Heavy metal contamination of natural foods is a serious health issue: a review. *Sustainability*, 14(1), 161.
10. Raj, D., Maiti, S.K., 2019. Sources, toxicity, and remediation of mercury: an essence review. *Environmental Monitoring and Assessment*, 191(9), 566.
11. Rahman, Z., Singh, V.P., 2019. The relative impact of toxic heavy metals (THMs) (arsenic (As), cadmium (Cd), chromium (Cr)(VI), mercury (Hg), and lead (Pb)) on the total environment: an overview. *Environmental Monitoring and Assessment*, 191(7), 419.

12. Wu, Y.S., Osman, A.I., Hosny, M., Elgarahy, A.M., Eltaweil, A.S., Rooney, D.W., Chen, Z., Rahim, N.S., Sekar, M., Gopinath, S.C., Mat Rani, N.N., 2024. The toxicity of mercury and its chemical compounds: molecular mechanisms and environmental and human health implications: a comprehensive review. *ACS Omega*, 9(5), 5100–5126.
13. King, D.C., Watts, M.J., Hamilton, E.M., Mortimer, R., Kilgour, D.P., Di Bonito, M., 2023. The present and potential future of aqueous mercury preservation: a review. *Environmental Science: Processes & Impacts*, 25(3), 351–363.
14. Roychoudhury, A., Chakraborty, S., 2020. Cellular and molecular phytotoxicity of lead and mercury. In: *Cellular and Molecular Phytotoxicity of Heavy Metals*. Springer International Publishing, Cham, pp. 373–387.
15. Rajendran, S., Kamaludeen, S.P., Subramanian, A., 2024. Antioxidant defense mechanism in plants exposed to mercury toxicity: response, tolerance and remediation. In: *Mercury Toxicity Mitigation: Sustainable Nexus Approach*. Springer Nature Switzerland, Cham, pp. 225–245.
16. Ahmad, J., Ali, A.A., Iqbal, M., Ahmad, A., Qureshi, M.I., 2022. Proteomics of mercury-induced responses and resilience in plants: a review. *Environmental Chemistry Letters*, 20(5), 3335–3355.
17. Mulenga, C., Clarke, C., Meincken, M., 2020. Physiological and growth responses to pollutant-induced biochemical changes in plants: a review. *Pollution*, 6(4), 827–848.
18. Ravikesavan, R., Jeeva, G., Jency, J.P., Muthamilarasan, M., Francis, N., 2023. Kodo millet (*Paspalum scrobiculatum* L.). In: *Neglected and Underutilized Crops*. Academic Press, pp. 279–304.
19. Dey, S., Saxena, A., Kumar, Y., Maity, T., Tarafdar, A., 2022. Understanding the antinutritional factors and bioactive compounds of kodo millet (*Paspalum scrobiculatum*) and little millet (*Panicum sumatrense*). *Journal of Food Quality*, 2022(1), 1578448.
20. Lee, J., Kwak, M., Chang, Y.K., Kim, D., 2021. Green solvent-based extraction of chlorophyll a from *Nannochloropsis* sp. using 2,3-butanediol. *Separation and Purification Technology*, 276, 119248.
21. Rupa, S.A., Patwary, M.A., Matin, M.M., Ghann, W.E., Uddin, J., Kazi, M., 2023. Interaction of mercury species with proteins: towards possible mechanism of mercurial toxicology. *Toxicology Research*, 12(3), 355–368.
22. Bjørklund, G., Crisponi, G., Nurchi, V.M., Cappai, R., Buha Djordjevic, A., Aaseth, J., 2019. A review on coordination properties of thiol-containing chelating agents towards mercury, cadmium, and lead. *Molecules*, 24(18), 3247.
23. Pál, M., Janda, T., Szalai, G., 2018. Interactions between plant hormones and thiol-related heavy metal chelators. *Plant Growth Regulation*, 85(2), 173–185.
24. Nguyen, T.Q., Sesin, V., Kisiala, A., Emery, N.R., 2021. Phytohormonal roles in plant responses to heavy metal stress: implications for using macrophytes in phytoremediation of aquatic ecosystems. *Environmental Toxicology and Chemistry*, 40(1), 7–22.
25. Mussina, A., Baitasheva, G., Rakhimova, Z., Raimbekova, B., Gubasheva, B.E., Medeuova, G., Baymurzina, Z., Tynyshbek, D., 2025. Evaluation of tree species, *Aesculus hippocastanum* as a phytoremediator in conditions of artificial soil contamination. *Caspian Journal of Environmental Sciences*, 23(3), 707–720.

26. Kurepa, J., Smalle, J.A., 2022. Auxin/cytokinin antagonistic control of the shoot/root growth ratio and its relevance for adaptation to drought and nutrient deficiency stresses. *International Journal of Molecular Sciences*, 23(4), 1933.
27. Souri, Z., Cardoso, A.A., da Silva, C.J., de Oliveira, L.M., Dari, B., Sihi, D., Karimi, N., 2019. Heavy metals and photosynthesis: recent developments. In: *Photosynthesis, Productivity and Environmental Stress*, pp. 107–134.
28. Wu, Y., Liao, W., Dawuda, M.M., Hu, L., Yu, J., 2019. 5-Aminolevulinic acid (ALA) biosynthetic and metabolic pathways and its role in higher plants: a review. *Plant Growth Regulation*, 87(2), 357–374.
29. Sandhi, A., Siddique, A.B., Vithanage, M., 2023. Mercury toxicity: plant response and tolerance. In: *Heavy Metal Toxicity and Tolerance in Plants: A Biological, Omics, and Genetic Engineering Approach*, pp. 349–371.
30. Garcia-Caparrós, P., De Filippis, L., Gul, A., Hasanuzzaman, M., Ozturk, M., Altay, V., Lao, M.T., 2021. Oxidative stress and antioxidant metabolism under adverse environmental conditions: a review. *Botanical Review*, 87(4), 421–466.
31. Safari, F., Akramian, M., Salehi-Arjmand, H., Khadivi, A., 2019. Physiological and molecular mechanisms underlying salicylic acid-mitigated mercury toxicity in lemon balm (*Melissa officinalis* L.). *Ecotoxicology and Environmental Safety*, 183, 109542.
32. Ding, W., Zhang, J., Wu, S.C., Zhang, S., Christie, P., Liang, P., 2019. Responses of the grass *Paspalum distichum* L. to Hg stress: a proteomic study. *Ecotoxicology and Environmental Safety*, 183, 109549.
33. Shao, R., Zhang, J., Shi, W., Wang, Y., Tang, Y., Liu, Z., Sun, W., Wang, H., Guo, J., Meng, Y., Kang, G., 2022. Mercury stress tolerance in wheat and maize is achieved by lignin accumulation controlled by nitric oxide. *Environmental Pollution*, 307, 119488.
34. Yadav, V., Wang, Z., Wei, C., Amo, A., Ahmed, B., Yang, X., Zhang, X., 2020. Phenylpropanoid pathway engineering: an emerging approach towards plant defense. *Pathogens*, 9(4), 312.
35. Rui, Y., Dinneny, J.R., 2020. A wall with integrity: surveillance and maintenance of the plant cell wall under stress. *New Phytologist*, 225(4), 1428–1439.
36. Malik, B., Pirzadah, T.B., Tahir, I., Ul Rehman, R., 2019. Growth and physiological responses in chicory towards mercury induced in vitro oxidative stress. *Plant Physiology Reports*, 24(2), 236–248.
37. Balali-Mood, M., Naseri, K., Tahergorabi, Z., Khazdair, M.R., Sadeghi, M., 2021. Toxic mechanisms of five heavy metals: mercury, lead, chromium, cadmium, and arsenic. *Frontiers in Pharmacology*, 12, 643972.
38. Kumar, A., Khushboo, Pandey, R., Sharma, B., 2020. Modulation of superoxide dismutase activity by mercury, lead, and arsenic. *Biological Trace Element Research*, 196(2), 654–661.
39. Hang, X., Gan, F., Chen, Y., Chen, X., Wang, H., Du, C., Zhou, J., 2018. Evaluation of mercury uptake and distribution in rice (*Oryza sativa* L.). *Bulletin of Environmental Contamination and Toxicology*, 100(3), 451–456.
40. Cruz, Y., Villar, S., Gutiérrez, K., Montoya-Ruiz, C., Gallego, J.L., Delgado, M.D., Saldarriaga, J.F., 2021. Gene expression and morphological responses of *Lolium perenne* L. exposed to cadmium (Cd²⁺) and mercury (Hg²⁺). *Scientific Reports*, 11(1), 11257.

41. Chen, Y.T., Wang, Y., Yeh, K.C., 2017. Role of root exudates in metal acquisition and tolerance. *Current Opinion in Plant Biology*, 39, 66–72.